

Article

Development of Piperazine- and Oxazine-Linked Pyrimidines as p65 Subunit Binders of NF- κ B in Human Breast Cancer Cells

Akshay Ravish ^{1,†}, Bhanuprakash C. Narasimhachar ^{2,†}, Zhang Xi ³, Divakar Vishwanath ¹, Arunkumar Mohan ¹, Santosh L. Gaonkar ⁴, Paduvalahippe Gowdegowda Chandrashekara ², Kwang Seok Ahn ⁵, Vijay Pandey ^{6,7}, Peter E. Lobie ^{3,6,7,*}, and Basappa Basappa ^{1,*}

- ¹ Laboratory of Chemical Biology, Department of Studies in Organic Chemistry, University of Mysore, Mysore 570006, Karnataka, India; akshayrv533@gmail.com (A.R.); divakardivi166@gmail.com (D.V.); arunmysore3@gmail.com (A.M.)
- ² Department of Chemistry, Yuvaraja's College, University of Mysore, Mysuru 570005, Karnataka, India; bhanuprakashcn28@gmail.com (B.C.N.); pgc2031@gmail.com (P.G.C.)
- ³ Shenzhen Bay Laboratory, Shenzhen 518055, China; zhangxi@szbl.ac.cn
- ⁴ Department of Chemistry, Manipal Institute of Technology, Manipal Academy of Higher Education, Manipal 576104, Karnataka, India; sl.gaonkar@manipal.edu
- ⁵ Department of Science in Korean Medicine, Kyung Hee University, 24 Kyungheedaero, Dongdaemungu, Seoul 02447, Republic of Korea; ksahn@khu.ac.kr
- ⁶ Tsinghua Berkeley Shenzhen Institute, Tsinghua Shenzhen International Graduate School, Tsinghua University, Shenzhen 518055, China; vijay.pandey@sz.tsinghua.edu.cn
- ⁷ Institute of Biopharmaceutical and Health Engineering, Tsinghua Shenzhen International Graduate School, Tsinghua University, Shenzhen 518055, China
- * Correspondence: pelobie@sz.tsinghua.edu.cn (P.E.L.); salundibasappa@gmail.com (B.B.)
- † These authors contributed equally to this work.



Citation: Ravish, A.; Narasimhachar, B.C.; Xi, Z.; Vishwanath, D.; Mohan, A.; Gaonkar, S.L.; Chandrashekara, P.G.; Ahn, K.S.; Pandey, V.; Lobie, P.E.; et al. Development of Piperazine- and Oxazine-Linked Pyrimidines as p65 Subunit Binders of NF- κ B in Human Breast Cancer Cells.

Biomedicines **2023**, *11*, 2716.

<https://doi.org/10.3390/biomedicines11102716>

Academic Editor: Luca Gentilucci

Received: 27 June 2023

Revised: 1 September 2023

Accepted: 12 September 2023

Published: 6 October 2023



Copyright: © 2023 by the authors. Licensee MDPI, Basel, Switzerland. This article is an open access article distributed under the terms and conditions of the Creative Commons Attribution (CC BY) license (<https://creativecommons.org/licenses/by/4.0/>).

Abstract: Nuclear factor kappa B (NF- κ B) is a potential therapeutic target in breast cancer. In the current study, a new class of oxazine- and piperazine-linked pyrimidines was developed as inhibitors of NF- κ B, overcoming the complexity of the oxazine structure found in nature and enabling synthesis under laboratory conditions. Among the series of synthesized and tested oxazine-pyrimidine and piperazine-pyrimidine derivatives, compounds **3a** and **5b** inhibited breast cancer cell (MCF-7) viability with an IC₅₀ value of 9.17 and 6.29 μ M, respectively. *In silico* docking studies showed that the pyrimidine ring of **3a** and the 4-methoxybenzyl thiol group of **5b** could strongly bind the p65 subunit of NF- κ B, with the binding energies -9.32 and -7.32 kcal mol⁻¹. Furthermore, compounds **3a** and **5b** inhibited NF- κ B in MCF-7 breast cancer cells. In conclusion, we herein report newer structures that target NF- κ B in BC cells.

Keywords: oxazines; piperazines; pyrimidines; NF- κ B; Alamar Blue assay; molecular docking; apoptosis assay; western blot

1. Introduction

Breast cancer has become the world's second-leading cause of cancer-related death (lung cancer being first), accounting for about 13.7% of all cancer-related fatalities [1,2]. Nuclear factor kappa B (NF- κ B) signaling has been extensively studied for over three decades since its discovery by Sen et al. [3]. Recent evidence confirms that activation of NF- κ B promotes human breast cancer progression. For that reason, NF- κ B has emerged as a potential therapeutic target in breast cancer treatment [4,5]. The NF- κ B family comprises five transcription factors: NF- κ B1/p50, NF- κ B2/p52, RelA/p65, RelB, and c-Rel [6]. These factors can either hetero- or homodimerize to produce NF- κ B complexes. The p65 subunit of NF- κ B is a critical component in activating and regulating downstream target genes. Most of them are found in the cytoplasm of dormant cells; when they are activated, they

move to the nucleus for transcription, which in turn causes hundreds of genes to be activated or repressed directly, indirectly, or both [7].

NF- κ B is activated by viral and bacterial antigens, UV radiation, and cytokines such as IL-2 and TNF- α . The nuclear factor supports cell proliferation, apoptosis, and immunological responses to infection and inflammation. However, system disruption is associated with disorders including cancer, immunosuppression, and chronic inflammation [8]. NF- κ B activation promotes cell survival by inhibiting apoptosis (programmed cell death). It controls the expression of anti-apoptotic proteins that aid cancer cells to avoid cell death and promote their survival, including Bcl-2, Bcl-xL, and inhibitors of apoptosis (IAPs) [9]. Additionally, NF- κ B signaling promotes cell proliferation by increasing the expression of genes essential for cell cycle progression, including cyclins and cyclin-dependent kinases (CDKs) [10,11].

It has been demonstrated that several drugs, including aspirin, sodium salicylate, and dexamethasone, decrease NF- κ B activation by preventing the breakdown of I κ B [12–14]. The current anti-TNF- α antibodies approved by the FDA include infliximab, adalimumab, and golimumab [15]. Ongoing research is being conducted to produce innovative small molecules that target the NF- κ B pathway. New compounds and therapeutic strategies are continually explored and may emerge as potential candidates for further investigation in breast cancer treatment [16]. Piperazine derivatives, among other heterocycles, were discovered as promising anti-cancer agents [17–20], and many of the FDA-approved drugs include piperazines [21]. Novel piperazine compounds could suppress NF- κ B translocation to the nucleus [22] and inhibit NF- κ B by decreasing TNF- α levels [23]. Pyrimidines also play a vital role in anti-cancer drug discovery [24]. Ibudilast, spebrutinib, and dasatinib are a few pyrimidine-based drugs (Figure 1) that block the NF- κ B pathway [25]. Furthermore, many reports have shown that oxazine derivatives might emerge as promising anti-cancer agents [26,27], and that they are potential candidates for NF- κ B inhibitors [28–30]. The oxazine derivative compound **1** decreased the DNA binding ability of NF- κ B and NF- κ B-dependent luciferase expression and I κ B α phosphorylation in hepatocellular carcinoma (HCC) and HCT116 cells. Furthermore, treatment of inflammatory bowel disease (IBD)-induced mice with compound **1** decreased myeloperoxidase activity in colonic extracts and modulated the colon length and serum levels of cytokines such as TNF- α , IFN- γ , IL-6, IL-1 β , and IL-10 [31,32]. Similarly, compound **2** inhibited proliferation in HepG2, HCCLM3, and Huh-7 cells in a dose- and time-dependent manner, as well as decreased p65 subunit DNA binding capacity, p65 phosphorylation, and the consequent production of NF- κ B-dependent luciferase gene expression in several HCC cell lines [33]. From the abovementioned discoveries, Lys28 was observed to be the active site of the p65 subunit in NF- κ B. Benzimidazole-clubbed pyrimidines (**3**) were demonstrated as covalent inhibitors of cysteine in NF- κ B inducing kinase [34]. Pyrido-pyrimidine (**5**) inhibited NF- κ B activation by suppressing I κ B α and LPS-induced phosphorylation levels of p65 and Akt, and by indirectly suppressing the MAPK signaling pathway [35], and pyralopyridine (**5**)-substituted pyrimidines were discovered as NF- κ B transcription inhibitors [36].

Herein, we have synthesized novel oxazine- and piperazine-linked pyrimidine small molecules using thiouracils active in breast cancer cells (MCF-7) that target NF- κ B. Alamar Blue assay showed that newly synthesized compounds **3a** and **5b** produced an IC₅₀ of 9.17 and 6.29 μ M in MCF-7 cells. In silico docking studies showed that compounds **3a** and **5b** exhibited -9.32 and -7.32 kcal mol⁻¹ binding energy. Lys28 of the p65 subunit of NF- κ B and the pyrimidine ring of **3a** and 4-methoxy benzyl thiol group of **5b** showed strong pi-alkyl interactions.

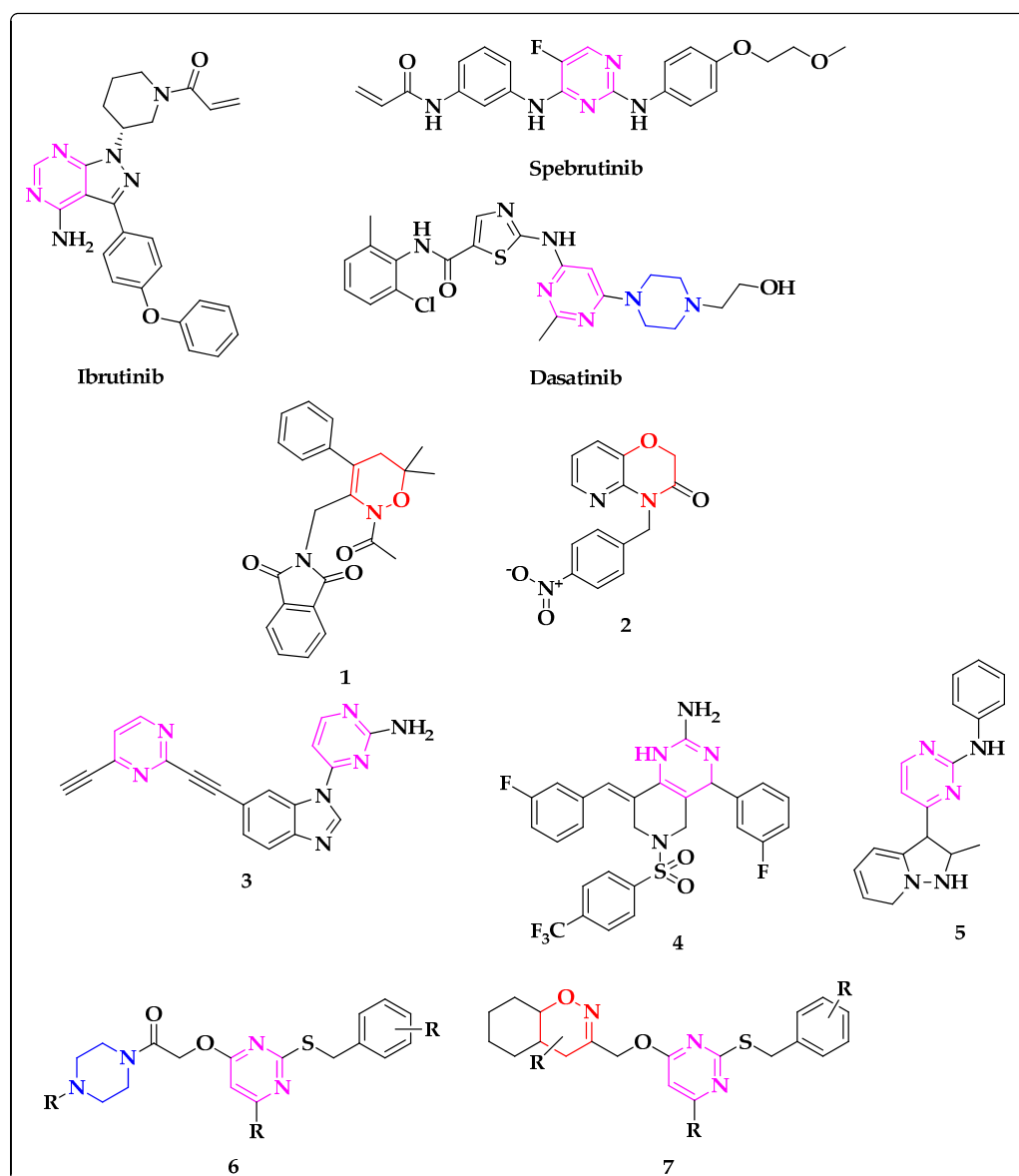


Figure 1. Marketed drugs and potent inhibitors of NF- κ B. (1, 2) bearing oxazines (red), (3, 4, 5) pyrimidine (pink) motifs are reported inhibitors. 6 and 7 are newly synthesized piperazine (blue)– and oxazine (red)–linked pyrimidine (pink) derivatives as NF- κ B inhibitors.

2. Materials and Methods

All chemicals and solvents were purchased from Sigma-Aldrich (Bangalore, India). The completion of the reaction was monitored by pre-coated silica gel TLC plates. An Agilent mass spectrophotometer was used to record the mass of the synthesized compounds. ^1H and ^{13}C NMR (Santa Clara, CA, USA) were recorded on Agilent and Jeol NMR spectrophotometers (400 MHz). TMS was used as an internal standard, and DMSO was used as a solvent. Chemical shifts were expressed as ppm.

2.1. General Procedure for the Synthesis of Oxazine and Piperazine Clubbed Pyrimidine Derivatives

2.1.1. Synthesis of Compound 2

Substituted thiouracils (1) (1.0 mmol) and various benzyl chlorides (1.2 mmol) were refluxed with KOH (1.2 mmol) in EtOH: H₂O (1:1) as a solvent for 1 h. After the completion of the reaction, the solid mass was filtered off and washed with aqueous NaHCO₃ solution and water, yielding compound 2.

2.1.2. Synthesis of Compound 3

Compound 2 (1.0 mmol), substituted oxazines (1.0 mmol), and K_2CO_3 (2 mmol) were refluxed in acetone for 2–3 h. After the completion of the reaction, the crude reaction mass was extracted to ethyl acetate (25 mL \times 3). The combined organic layer was distilled under reduced pressure and purified by column chromatography using ethyl acetate and hexane.

2.1.3. Synthesis of Compounds 4/5

Compound 2 (1.0 mmol) was treated with *tert*-butyl bromoacetate (1.2 mmol) and K_2CO_3 (1.5 mmol) in refluxing DMF. After the completion of the reaction, reaction mass was extracted with ethyl acetate and the crude product was purified by column chromatography, yielding compound 4. The solution of 4 in trifluoroacetic acid was stirred at room temperature for 1–2 h. After completion of the reaction, it was quenched with sodium bicarbonate and extracted with ethyl acetate. The solid formed was filtered off and dried, yielding compound 5.

2.1.4. Synthesis of Compound 5a

Compound 4 (1.0 mmol) was treated with 2-((2-((4-methoxybenzyl)thio)-pyrimidin-4-yl)oxy)-1-(4-methyl piperazin-1-yl)ethanone with EDC.HCl and DMAP as catalysts in basic conditions in DCM as solvent under nitrogen atmosphere for 2 h. After completion of the reaction, the crude mass was extracted with ethyl acetate, and the combined organic layer was distilled off and purified through column chromatography.

2.1.5. Synthesis of Compound 5b/f/k/o

Compound 4 (1.0 mmol) was treated with acetyl piperazines (1.2 mmol) with EDC.HCl and DMAP as catalysts in basic conditions in DCM as solvent under nitrogen atmosphere for 2 h. After completion of the reaction, the crude mass was extracted with ethyl acetate, and the combined organic layer was distilled off and purified through column chromatography.

2.1.6. Synthesis of Compounds 5d/h/m/q

Compound 4 (1.0 mmol) was treated with *N*-*boc* piperazines (1.2 mmol) with EDC.HCl and DMAP were used as catalysts in basic conditions in DCM as solvent under nitrogen atmosphere for 2 h. After completion of the reaction, the crude mass was extracted with ethyl acetate, and the combined organic layer was distilled off and purified through column chromatography, yields 5d, 5h, 5m, or 5q.

2.1.7. Synthesis of Compounds 5c/g/l/p

Compounds 5d, 5h, 5m, or 5q (1.0 mmol) were treated with trifluoroacetic acid. After completion of the reaction, the crude mass was neutralized with K_2CO_3 and extracted with ethyl acetate. The combined organic layer was distilled off and purified through column chromatography, yielding compounds 5c, 5g, 5l, or 5p, respectively.

2.1.8. Synthesis of Compounds 5e/i/j/n

Compounds 5c, 5g, 5l, or 5p (1 mmol) were treated with 5-bromopyridine-2-carboxylic acid (1.2 mmol) with EDC. HCl and DMAP were used as catalysts in basic conditions in DCM as solvent under nitrogen atmosphere for 2 h. After completion of the reaction, the crude mass was extracted with ethyl acetate, and the combined organic layer was distilled off and purified through column chromatography, yielding compounds 5e, 5i, 5j, or 5n, respectively.

2.1.9. 6,6-Dimethyl-3-(((2-((3-methylbenzyl)thio)pyrimidin-4-yl)oxy)methyl)-4-phenyl-5,6-dihydro-4H-1,2-oxazine (3a)

Yellow solid; MP: 120–122 °C; 1H NMR (400 MHz, DMSO) δ 8.34 (s, 1H), 7.34–7.12 (m, 8H), 7.07 (s, 1H), 6.59 (s, 1H), 4.69 (s, 2H), 4.26 (s, 2H), 3.65 (s, 1H), 2.27 (s, 3H), 2.11 (s, 1H), 1.79 (t, $J = 12.4, 24.8$ Hz, 1H), 1.29 (s, 3H), 1.21 (s, 3H); ^{13}C NMR (100 MHz, DMSO) δ 170.48, 167.99, 158.56, 153.96, 139.95, 138.00, 137.96, 129.86, 129.25, 128.79, 128.75, 128.19,

127.62, 126.31, 104.34, 79.64, 75.07, 65.73, 37.45, 34.58, 28.45, 22.94, 21.40; Calculated for $C_{25}H_{27}N_3O_2S$: actual = 433.5658, found = 434.1108 $[M + 1]^+$.

2.1.10. 4-(4-Methoxyphenyl)-3-(((2-((3-methylbenzyl)thio)pyrimidin-4-yl)oxy)methyl)-4a,5,6,7,8,8a-hexahydro-4H-benzo[e][1,2]oxazine (**3b**)

Yellow solid; MP: 128–130 °C; 1H NMR (400 MHz, DMSO) δ 8.33 (s, 1H), 7.25–6.98 (m, 6H), 6.88 (s, 2H), 6.56 (s, 1H), 4.87 (s, 2H), 4.26 (s, 2H), 3.91 (s, 1H), 3.69 (s, 3H), 3.28 (s, 1H), 2.25 (s, 3H), 1.88 (s, 1H), 1.61 (s, 2H), 1.38–1.22 (m, 6H); ^{13}C NMR (100 MHz, DMSO) δ 170.60, 168.12, 158.66, 158.63, 151.58, 138.00, 137.84, 133.15, 129.85, 129.62, 128.74, 128.17, 126.30, 114.55, 104.30, 69.03, 66.10, 55.43, 42.73, 38.67, 34.66, 28.99, 27.33, 24.68, 21.34, 20.24; Calculated for $C_{28}H_{31}N_3O_3S$: actual = 489.2086, found = 490.2234 $[M + 1]^+$.

2.1.11. 4-(4-Chlorophenyl)-6,6-dimethyl-3-(((2-((3-methylbenzyl)thio)pyrimidin-4-yl)oxy)methyl)-5,6-dihydro-4H-1,2-oxazine (**3c**)

Yellow solid; MP: 130–132 °C; 1H NMR (400 MHz, DMSO) δ 8.34 (s, 1H), 7.32–7.17 (m, 7H), 7.07 (s, 1H), 6.57 (s, 1H), 4.72 (s, 2H), 4.27 (s, 2H), 3.69 (s, 1H), 2.28 (s, 3H), 2.11 (s, 1H), 1.77 (t, $J = 24, 12$ Hz, 1H), 1.29–1.20 (m, 6H); ^{13}C NMR (100 MHz, DMSO) δ 170.45, 167.92, 158.59, 153.53, 138.90, 138.02, 137.95, 132.26, 130.72, 129.87, 129.16, 128.80, 128.21, 126.31, 104.34, 75.14, 65.63, 36.74, 34.59, 28.41, 22.97, 21.40; Calculated for $C_{25}H_{26}ClN_3O_2S$: actual = 467.1434, found = 468.1520 $[M + 1]^+$.

2.1.12. 3-(((2-((4-Chlorobenzyl)thio)pyrimidin-4-yl)oxy)methyl)-6,6-dimethyl-4-phenyl-5,6-dihydro-4H-1,2-oxazine (**3d**)

Yellow solid; MP: 124–126 °C; 1H NMR (400 MHz, DMSO) δ 8.33 (s, 1H), 7.39–7.36 (m, 4H), 7.29 (s, 2H), 7.23 (s, 3H), 6.59 (s, 1H), 4.68 (s, 2H), 4.29 (s, 2H), 3.64 (s, 1H), 2.11 (s, 1H), 1.78 (t, $J = 12.4, 24.4$ Hz, 1H), 1.29 (s, 3H), 1.20 (s, 3H); ^{13}C NMR (100 MHz, DMSO) δ 170.12, 168.05, 158.61, 153.92, 139.95, 137.61, 132.08, 131.04, 129.25, 128.80, 128.75, 127.62, 104.48, 75.09, 65.76, 37.42, 33.69, 28.45, 22.95; Calculated for $C_{24}H_{24}ClN_3O_2S$: actual = 453.9843, found = 454.1443 $[M + 1]^+$.

2.1.13. 3-(((2-((4-Chlorobenzyl)thio)pyrimidin-4-yl)oxy)methyl)-4-(4-methoxyphenyl)-4a,5,6,7,8,8a-hexahydro-4H-benzo[e][1,2]oxazine (**3e**)

Yellow solid; MP: 110–112 °C; 1H NMR (400 MHz, DMSO) δ 8.34 (s, 1H), 7.37 (d, $J = 28.1$ Hz, 4H), 7.11 (s, 2H), 6.89 (s, 2H), 6.59 (s, 1H), 4.85 (s, 2H), 4.31 (s, 2H), 3.91 (s, 1H), 3.72 (s, 3H), 2.52 (s, 1H), 1.91 (s, 1H), 1.64 (s, 2H), 1.40–1.22 (m, 6H); ^{13}C NMR (100 MHz, DMSO) δ 170.20, 168.19, 158.72, 158.65, 151.59, 137.58, 133.19, 132.07, 131.03, 129.65, 128.77, 114.57, 104.47, 69.03, 66.16, 55.49, 42.67, 38.67, 33.73, 28.97, 27.31, 24.65, 20.25; Calculated for $C_{27}H_{28}ClN_3O_3S$: actual = 509.15, found = 510.1613 $[M + 1]^+$.

2.1.14. 3-(((2-((4-Chlorobenzyl)thio)pyrimidin-4-yl)oxy)methyl)-4-(4-chlorophenyl)-6,6-dimethyl-5,6-dihydro-4H-1,2-oxazine (**3f**)

Yellow solid; MP: 106–108 °C; 1H NMR (400 MHz, DMSO) δ 8.34 (s, 1H), 7.40–7.26 (m, 8H), 6.58 (s, 1H), 4.71 (s, 2H), 4.31 (s, 2H), 3.68 (s, 1H), 2.10 (s, 1H), 1.76 (s, 1H), 1.24–1.20 (m, 6H); ^{13}C NMR (100 MHz, DMSO) δ 170.12, 167.98, 158.62, 153.48, 138.90, 137.61, 132.26, 132.09, 131.04, 130.71, 129.16, 128.81, 104.47, 75.14, 65.67, 36.73, 33.70, 28.41, 22.98; Calculated for $C_{24}H_{23}Cl_2N_3O_2S$: actual = 488.4293, found = 490.0965 $[M + 1]^+$.

2.1.15. 3-(((2-((4-Fluorobenzyl)thio)pyrimidin-4-yl)oxy)methyl)-6,6-dimethyl-4-phenyl-5,6-dihydro-4H-1,2-oxazine (**3g**)

Yellow solid; MP: 136–138 °C; 1H NMR (400 MHz, DMSO) δ 8.34 (s, 1H), 7.41 (s, 2H), 7.26 (m, 5H), 7.12 (s, 2H), 6.60 (d, $J = 2.0$ Hz, 1H), 4.68 (s, 2H), 4.29 (s, 2H), 3.65 (s, 1H), 2.17–2.04 (m, 1H), 1.78 (t, $J = 12.4, 25.8$ Hz, 1H), 1.29 (s, 3H), 1.20 (s, 3H); ^{13}C NMR (100 MHz, DMSO) δ 170.25, 168.03, 162.91, 160.49, 158.59, 153.93, 139.96, 134.59, 134.56,

131.18, 131.10, 129.25, 128.75, 127.62, 115.73, 115.52, 104.44, 75.08, 65.75, 37.43, 33.67, 28.45, 22.94; Calculated for $C_{24}H_{24}FN_3O_2S$: actual = 437.5297, found = 438.1714 $[M + 1]^+$.

2.1.16. 3-(((2-((4-Fluorobenzyl)thio)pyrimidin-4-yl)oxy)methyl)-4-(4-methoxyphenyl)-4a,5,6,7,8,8a-hexahydro-4H-benzo[e][1,2]oxazine (**3h**)

$C_{27}H_{28}FN_3O_3S$; Yellow solid; MP: 142–144 °C; 1H NMR (400 MHz, DMSO) δ 8.35 (s, 1H), 7.42 (s, 2H), 7.11 (s, 4H), 6.89 (s, 2H), 6.59 (s, 1H), 4.85 (s, 2H), 4.30 (s, 2H), 3.91 (s, 1H), 3.71 (s, 3H), 3.28 (s, 1H), 1.90 (d, $J = 10.0$ Hz, 1H), 1.64 (s, 2H), 1.40–1.24 (m, 6H); ^{13}C NMR (100 MHz, DMSO) δ 170.33, 168.18, 162.90, 160.48, 158.73, 158.65, 151.62, 134.54, 134.51, 133.19, 131.19, 131.11, 129.66, 115.71, 115.50, 114.57, 104.45, 69.05, 66.12, 55.49, 42.65, 36.68, 33.71, 28.96, 27.31, 24.64, 20.26; Calculated for $C_{27}H_{28}FN_3O_3S$: actual = 493.5929, found = 494.1919 $[M + 1]^+$.

2.1.17. 4-(4-Chlorophenyl)-3-(((2-((4-fluorobenzyl)thio)pyrimidin-4-yl)oxy)methyl)-6,6-dimethyl-5,6-dihydro-4H-1,2-oxazine (**3i**)

$C_{24}H_{23}ClFN_3O_2S$; Yellow solid; MP: 120–122 °C; 1H NMR (400 MHz, DMSO) δ 8.34 (s, 1H), 7.42 (s, 2H), 7.29 (m, 4H), 7.13 (s, 2H), 6.58 (s, 1H), 4.71 (s, 2H), 4.31 (s, 2H), 3.69 (s, 1H), 2.10 (s, 1H), 1.76 (t, $J = 11.6, 23.6$ Hz, 1H), 1.29–1.20 (m, 6H); ^{13}C NMR (100 MHz, DMSO) δ 170.24, 167.95, 162.91, 160.49, 158.61, 153.50, 138.90, 134.58, 134.55, 132.26, 131.19, 131.11, 130.72, 129.16, 115.74, 115.53, 104.43, 75.14, 65.64, 36.72, 33.67, 28.40, 22.96; Calculated for $C_{24}H_{23}ClFN_3O_2S$: actual = 471.12, found = 472.1271 $[M + 1]^+$.

2.1.18. 3-(((2-((4-Fluorobenzyl)thio)-6-methylpyrimidin-4-yl)oxy)methyl)-6,6-dimethyl-4-phenyl-5,6-dihydro-4H-1,2-oxazine (**3j**)

Yellow solid; MP: 130–132 °C; 1H NMR (400 MHz, DMSO) δ 7.41 (s, 2H), 7.30–7.22 (m, 5H), 7.12 (s, 2H), 6.45 (s, 1H), 4.66 (s, 2H), 4.27 (s, 2H), 3.62 (s, 1H), 2.31 (s, 3H), 2.11 (s, 1H), 1.77 (t, $J = 12, 23.2$ Hz, 1H), 1.29 (s, 3H), 1.19 (s, 3H); ^{13}C NMR (100 MHz, DMSO) δ 169.49, 168.62, 168.54, 162.86, 160.44, 154.11, 140.01, 134.85, 134.82, 131.22, 131.14, 129.26, 128.73, 127.60, 115.68, 115.46, 102.72, 75.05, 65.68, 37.40, 33.58, 28.44, 23.65, 22.89; Calculated for $C_{25}H_{26}FN_3O_2S$: actual = 451.5562, found = 452.1881 $[M + 1]^+$.

2.1.19. 3-(((2-((4-Fluorobenzyl)thio)-6-methylpyrimidin-4-yl)oxy)methyl)-4-(4-methoxy-phenyl)-4a,5,6,7,8,8a-hexahydro-4H-benzo[e][1,2]oxazine (**3k**)

Yellow solid; MP: 124–126 °C; 1H NMR (400 MHz, DMSO) δ 7.42 (s, 2H), 7.10 (s, 4H), 6.88 (s, 2H), 6.44 (s, 1H), 4.83 (s, 2H), 4.27 (s, 2H), 3.90 (s, 1H), 3.71 (s, 3H), 3.25 (s, 1H), 2.30 (s, 3H), 1.90 (d, $J = 10.0$ Hz, 1H), 1.63 (d, $J = 7.2$ Hz, 2H), 1.40–1.24 (m, 6H); ^{13}C NMR (100 MHz, DMSO) δ 169.53, 168.78, 168.64, 162.84, 160.43, 158.62, 151.81, 134.78, 134.74, 133.16, 131.19, 131.11, 129.64, 115.64, 115.43, 114.54, 102.73, 69.03, 65.99, 55.46, 42.62, 38.61, 33.62, 28.95, 27.29, 24.62, 23.58, 20.22; Calculated for $C_{28}H_{30}FN_3O_3S$: actual = 507.6195, found = 508.2078 $[M + 1]^+$.

2.1.20. 4-(4-Chlorophenyl)-3-(((2-((4-fluorobenzyl)thio)-6-methylpyrimidin-4-yl)oxy)methyl)-6,6-dimethyl-5,6-dihydro-4H-1,2-oxazine (**3l**)

Yellow solid; MP: 100–102 °C; 1H NMR (400 MHz, DMSO) δ 7.42 (s, 2H), 7.33 (s, 2H), 7.25 (s, 2H), 7.12 (s, 2H), 6.42 (s, 1H), 4.69 (d, $J = 11.6$ Hz, 2H), 4.28 (s, 2H), 3.66 (s, 1H), 2.31 (s, 3H), 2.10 (s, 1H), 1.75 (t, $J = 12.4, 24.4$ Hz, 1H), 1.29 (s, 3H), 1.19 (s, 3H); ^{13}C NMR (100 MHz, DMSO) δ 169.48, 168.65, 168.47, 162.87, 160.45, 153.69, 138.95, 134.82, 132.24, 131.21, 131.13, 130.70, 129.16, 115.68, 115.47, 102.70, 75.11, 65.61, 36.73, 33.60, 28.40, 23.67, 22.92; Calculated for $C_{25}H_{25}ClFN_3O_2S$: actual = 485.13, found = 486.1400 $[M + 1]^+$.

2.1.21. 1,1'-(Piperazine-1,4-diyl)bis(2-(((2-((4-methoxybenzyl)thio)pyrimidin-4-yl)oxy)ethan-1-one) (**5a**)

White solid; MP: 150–152 °C; 1H NMR (400 MHz, $CDCl_3$): δ 8.30 (d, $J = 5.2$ Hz, 1H), 7.32 (d, $J = 7.6$ Hz, 2H), 6.85 (d, $J = 8.0$ Hz, 2H), 6.55 (d, $J = 5.2$ Hz, 1H), 4.90 (s, 2H), 4.30 (s,

2H), 3.79 (s, 3H), 3.75 (s, 7H); ^{13}C NMR (400 MHz, CDCl_3) δ 171.5, 168.7, 167.7, 159.0, 158.0, 130.1, 129.2, 114.1, 103.9, 62.6, 55.4, 52.3, 34.9.

2.1.22. 1-(4-Acetylpiperazin-1-yl)-2-((2-((4-methoxybenzyl)thio)pyrimidin-4-yl)oxy)ethanone (**5b**)

Yellow thick mass; ^1H NMR (400 MHz, CDCl_3) δ 8.29 (d, $J = 5.4$ Hz, 1H), 7.30 (d, $J = 8.0$ Hz, 2H), 6.83 (d, $J = 8.0$ Hz, 2H), 6.56 (d, $J = 5.5$ Hz, 1H), 4.99 (s, 2H), 4.32 (s, 2H), 3.78 (s, 3H), 3.51 (d, $J = 68.9$ Hz, 8H), 2.09 (s, 3H); ^{13}C NMR (100 MHz, CDCl_3): δ 171.3, 169.4, 167.7, 165.9, 159.0, 157.9, 130.1, 129.3, 114.1, 104.1, 63.1, 55.4, 46.0, 44.7, 42.0, 41.3, 34.8, 21.4.

2.1.23. Tert-butyl 4-(2-((2-((4-Methoxybenzyl)thio)pyrimidin-4-yl)oxy)acetyl)piperazine-1-carboxylate (**5c**)

White solid; MP: 160–162 °C; ^1H NMR (400 MHz, CDCl_3) δ 8.28 (d, $J = 5.7$ Hz, 1H), 7.30 (d, $J = 8.4$ Hz, 2H), 6.82 (d, $J = 8.5$ Hz, 2H), 6.56 (d, $J = 5.7$ Hz, 1H), 4.98 (s, 2H), 4.31 (s, 2H), 3.77 (s, 3H), 3.57 (s, 2H), 3.42 (d, $J = 18.1$ Hz, 6H), 1.45 (s, 9H); ^{13}C NMR (100 MHz, CDCl_3) δ 170.7, 167.1, 165.0, 158.3, 157.3, 153.9, 129.5, 128.6, 113.5, 103.5, 79.9, 62.6, 54.8, 44.2, 41.3, 34.3, 27.8; MS: 474.58, $m/z = 475.12$ [$M + 1$] $^+$.

2.1.24. 1-(4-(5-Bromopicolinoyl)piperazin-1-yl)-2-((2-((4-methoxybenzyl)thio)pyrimidin-4-yl)-oxy)ethanone (**5d**)

Yellow thick mass; ^1H NMR (400 MHz, CDCl_3) δ 8.629 (s, 1H), 8.289 (d, $J = 4.0$ Hz, 1H), 7.94 (d, $J = 6.8$ Hz, 1H), 7.73–7.58 (m, 1H), 7.30 (d, $J = 7.2$ Hz, 2H), 6.82 (d, $J = 6.4$ Hz, 2H), 6.60 (d, $J = 4.4$ Hz, 1H), 5.17–4.93 (s, 2H), 4.31 (s, 2H), 3.82–3.51 (m, 11H); ^{13}C NMR (100 MHz, CDCl_3) δ 170.7, 167.1, 165.0, 158.3, 157.6, 157.3, 150.9, 148.8, 139.4, 130.9, 129.5, 128.3, 122.0, 113.4, 103.4, 62.5, 54.8, 46.4, 42.0, 34.2; MS: 558.07, $m/z = 559.99$ [$M + 1$] $^+$.

2.1.25. 1-(4-Acetylpiperazin-1-yl)-2-((2-((3-methylbenzyl)thio)pyrimidin-4-yl)oxy)-ethanone (**5e**)

Yellow thick mass; ^1H NMR (500 MHz, CDCl_3) δ 8.29 (d, $J = 5.5$ Hz, 1H), 7.20–7.14 (m, 3H), 7.04 (d, $J = 5.5$ Hz, 1H), 6.56 (d, $J = 5.5$ Hz, 1H), 4.98 (s, 2H), 4.32 (s, 2H), 3.64–3.58 (m, 4H), 3.47–3.41 (m, 4H), 2.31 (s, 3H), 2.09 (s, 3H); ^{13}C NMR (100 MHz, CDCl_3) 171.2, 169.4, 167.7, 165.9, 157.9, 138.4, 137.2, 129.6, 128.5, 128.2, 125.9, 104.1, 63.0, 46.0, 44.7, 42.0, 41.2, 35.3, 29.8, 21.4.

2.1.26. 2-((2-((3-Methylbenzyl)thio)pyrimidin-4-yl)oxy)-1-(piperazin-1-yl)ethanone (**5f**)

Yellow thick mass; ^1H NMR (500 MHz, CDCl_3) δ 8.28 (d, $J = 5.5$ Hz, 1H), 7.25–7.17 (m, 3H), 7.08–7.01 (m, 1H), 6.56 (d, $J = 5.5$ Hz, 1H), 4.97 (s, 2H), 4.32 (s, 2H), 3.56 (s, 2H), 3.44 (s, 2H), 3.39 (s, 4H), 2.31 (s, 3H), 1.45 (s, 9H); ^{13}C NMR (100 MHz, CDCl_3) δ 171.3, 167.8, 165.6, 157.9, 154.5, 138.3, 137.2, 129.6, 128.5, 128.1, 126.0, 104.1, 80.5, 63.2, 44.8, 43.8, 41.9, 35.3, 28.4, 21.4.

2.1.27. Tert-butyl 4-(2-((2-((3-methylbenzyl)thio)pyrimidin-4-yl)oxy)acetyl)piperazine-1-carboxylate (**5g**)

White solid; MP: 166–168 °C; ^1H NMR (500 MHz, CDCl_3) δ 8.30 (d, $J = 6.0$ Hz, 1H), 7.20–7.17 (m, 3H), 7.05–7.03 (m, 1H), 6.56 (d, $J = 5.5$ Hz, 1H), 4.97 (s, 2H), 4.32 (s, 2H), 3.57 (s, 2H), 3.39 (s, 2H), 2.87–2.82 (m, 4H), 2.31 (s, 3H); ^{13}C NMR (100 MHz, CDCl_3) δ 171.2, 167.8, 165.4, 157.7, 138.3, 137.2, 129.7, 128.4, 128.0, 126.0, 104.1, 63.1, 45.9, 42.9, 35.3, 21.5.

2.1.28. 1-(4-(5-Bromopicolinoyl)piperazin-1-yl)-2-((2-((3-methylbenzyl)thio)pyrimidin-4-yl)-oxy)-ethanone (**5h**)

Yellow thick mass; ^1H NMR (500 MHz, CDCl_3) δ 8.62–8.59 (m, 1H), 8.28 (d, $J = 5.5$ Hz, 1H), 7.93 (dd, $J = 8.5, 2.0$ Hz, 1H), 7.61 (dd, $J = 16.0, 8.5$ Hz, 1H), 7.22–7.13 (m, 3H), 7.07–7.01 (m, 1H), 6.56 (d, $J = 5.5$ Hz, 1H), 5.01–4.97 (m, 2H), 4.32 (s, 2H), 3.81–3.72 (m, 4H), 3.64 (s, 2H), 3.54–3.49 (m, 2H), 2.30 (s, 3H); ^{13}C NMR (100 MHz, CDCl_3) δ 171.2, 167.7, 166.7, 165.8,

157.9, 151.4, 149.3, 149.2, 140.0, 138.3, 137.2, 129.6, 128.5, 128.2, 126.2, 126.0, 122.5, 104.1, 63.1, 47.1, 44.7, 42.6, 41.8, 35.3, 21.4.

2.1.29. 1-(4-(5-Bromopicolinoyl)piperazin-1-yl)-2-((2-((4-fluorobenzyl)thio)pyrimidin-4-yl)-oxy)-ethanone (**5i**)

Yellow thick mass; ^1H NMR (500 MHz, CDCl_3) δ 8.62–8.60 (m, 1H), 8.28 (d, $J = 6.0$ Hz, 1H), 7.93 (dd, $J = 8.4, 2.3$ Hz, 1H), 7.65–7.60 (m, 1H), 7.35–7.33 (m, 2H), 6.96 (t, $J = 9.0$ Hz, 2H), 6.56 (d, $J = 5.5$ Hz, 1H), 5.01–4.96 (m, 2H), 4.32 (s, 2H), 3.84–3.71 (m, 4H), 3.64 (s, 2H), 3.55–3.50 (m, 2H); ^{13}C NMR (100 MHz, CDCl_3): δ 170.9, 167.7, 166.7, 166.4, 165.8, 163.0, 161.1, 158.0, 157.9, 157.8, 151.4, 149.4, 140.1, 133.3, 130.5, 126.3, 126.0, 122.6, 115.6, 115.5, 115.3, 104.3, 104.2, 63.1, 47.1, 44.72, 42.7, 41.8, 34.5, 29.8.

2.1.30. 1-(4-Acetylpiperazin-1-yl)-2-((2-((4-fluorobenzyl)thio)pyrimidin-4-yl)oxy)-ethanone (**5j**)

Yellow thick mass; ^1H NMR (500 MHz, CDCl_3) δ 8.29 (d, $J = 5.5$ Hz, 1H), 7.35–7.33 (m, 2H), 6.97 (t, $J = 8.6$ Hz, 2H), 6.57 (d, $J = 5.5$ Hz, 1H), 4.98 (s, 3H), 4.32 (s, 3H), 3.60 (s, 5H), 3.42 (s, 5H), 2.10 (s, 4H); ^{13}C NMR (100 MHz, CDCl_3) δ 170.8, 169.4, 167.7, 165.8, 163.1, 161.1, 157.9, 133.3, 130.6, 130.5, 115.5, 115.4, 104.3, 77.4, 77.1, 76.9, 63.0, 45.9, 44.8, 42.0, 41.3, 34.4, 21.4.

2.1.31. 2-((2-((4-Fluorobenzyl)thio)pyrimidin-4-yl)oxy)-1-(piperazin-1-yl)ethanone (**5k**)

Yellow thick mass; ^1H NMR (500 MHz, CDCl_3) δ 8.26 (d, $J = 5.5$ Hz, 1H), 7.33 (dd, $J = 8.4, 5.5$ Hz, 2H), 6.95 (t, $J = 8.7$ Hz, 2H), 6.55 (d, $J = 5.5$ Hz, 1H), 4.95 (s, 2H), 4.31 (s, 2H), 3.54 (s, 2H), 3.37 (s, 2H), 2.84–2.80 (m, 4H), 2.05 (s, 1H); ^{13}C NMR (100 MHz, CDCl_3) δ 170.8, 167.9, 165.3, 163.0, 161.1, 157.8, 133.3, 133.3, 130.6, 130.5, 115.5, 115.4, 104.3, 63.2, 46.2, 46.0, 45.8, 43.1, 34.5.

2.1.32. Tert-butyl-4-(2-((2-((4-fluorobenzyl)thio)pyrimidin-4-yl)oxy)acetyl)piperazine-1-carboxylate (**5l**)

White solid; MP: 156–158 °C; ^1H NMR (500 MHz, CDCl_3) δ 8.28 (d, $J = 5.5$ Hz, 1H), 7.32 (d, $J = 8.0$ Hz, 2H), 7.25 (d, $J = 4.5$ Hz, 2H), 6.56 (d, $J = 5.5$ Hz, 1H), 4.96 (s, 2H), 4.31 (s, 2H), 3.56 (s, 2H), 3.45 (s, 2H), 3.39 (s, 4H), 1.45 (s, 9H); ^{13}C NMR (100 MHz, CDCl_3) δ 170.7, 167.8, 165.5, 157.9, 154.5, 136.2, 133.1, 130.3, 128.7, 104.3, 80.6, 63.2, 44.8, 41.9, 34.5, 28.4.

2.1.33. 1-(4-(5-Bromopicolinoyl)piperazin-1-yl)-2-((2-((4-chlorobenzyl)thio)pyrimidin-4-yl)-oxy)-ethanone (**5m**)

Yellow thick mass; ^1H NMR (500 MHz, CDCl_3) δ 8.61 (d, $J = 5.5$ Hz, 1H), 8.28 (d, $J = 5.5$ Hz, 1H), 7.94 (d, $J = 8.0$ Hz, 1H), 7.32–7.60 (m, 1H), 7.31 (d, $J = 8.0$ Hz, 2H), 7.24 (d, $J = 8.0$ Hz, 2H), 6.56 (d, $J = 4.8$ Hz, 1H), 5.00–4.95 (m, 2H), 4.31 (s, 2H), 3.82–3.73 (m, 4H), 3.64 (s, 2H), 3.55–3.50 (m, 2H); ^{13}C NMR (100 MHz, CDCl_3) δ 170.7, 167.7, 166.7, 165.7, 157.9, 151.5, 149.4, 140.0, 136.2, 133.0, 130.3, 128.7, 126.0, 122.6, 104.3, 63.1, 47.1, 45.3, 44.7, 42.6, 34.5.

2.1.34. 1-(4-Acetylpiperazin-1-yl)-2-((2-((4-chlorobenzyl)thio)pyrimidin-4-yl)oxy)-ethanone (**5n**)

Yellow thick mass; ^1H NMR (500 MHz, CDCl_3) δ 8.28 (d, $J = 5.5$ Hz, 1H), 7.32 (d, $J = 8.0$ Hz, 2H), 7.25 (d, $J = 4.8$ Hz, 2H), 6.57 (d, $J = 5.5$ Hz, 1H), 4.97 (s, 2H), 4.31 (s, 2H), 3.66–3.60 (m, 4H), 3.42 (s, 4H), 2.10 (s, 3H); ^{13}C NMR (100 MHz, CDCl_3) δ 170.7, 169.4, 167.8, 165.8, 158.0, 136.2, 133.1, 130.3, 128.7, 104.3, 63.0, 46.0, 44.8, 42.0, 41.3, 34.5, 21.4.

2.1.35. 2-((2-((4-Chlorobenzyl)thio)pyrimidin-4-yl)oxy)-1-(piperazin-1-yl)ethanone (**5o**)

Yellow thick mass; ^1H NMR (500 MHz, CDCl_3) δ 8.26 (d, $J = 5.5$ Hz, 1H), 7.31 (d, $J = 8.0$ Hz, 2H), 7.24 (d, $J = 8.0$ Hz, 2H), 6.56 (d, $J = 5.5$ Hz, 1H), 4.95 (s, 2H), 4.31 (s, 2H), 3.56 (s, 2H), 3.38 (s, 2H), 2.86–2.81 (m, 4H); ^{13}C NMR (100 MHz, CDCl_3) 170.7, 167.9, 165.3, 157.8, 136.2, 133.1, 130.3, 128.7, 104.3, 63.2, 46.0, 43.0, 34.6.

2.1.36. Tert-butyl-4-(2-((2-((4-chlorobenzyl)thio)pyrimidin-4-yl)oxy)acetyl)piperazine-1-carboxylate (**5p**)

White solid; MP: 160–170 °C; ^1H NMR (500 MHz, CDCl_3) δ 8.28 (d, $J = 5.5$ Hz, 1H), 7.32 (d, $J = 8.0$ Hz, 2H), 7.25 (d, $J = 4.5$ Hz, 2H), 6.56 (d, $J = 5.5$ Hz, 1H), 4.96 (s, 2H), 4.31 (s, 2H), 3.56 (s, 2H), 3.45 (s, 2H), 3.39 (s, 4H), 1.61 (s, 3H), 1.45 (s, 9H); ^{13}C NMR (100 MHz, CDCl_3) δ 170.7, 167.8, 165.6, 157.9, 154.5, 136.2, 133.1, 130.3, 128.7, 104.3, 80.6, 63.2, 44.9, 41.9, 34.5, 28.4.

2.2. Cell Viability Assay

MCF-7, MDAMB-231, BT549, and SUM159PT cells were purchased from Procell Life Science & Technology Co., Ltd. (Wuhan, China). All carcinoma cell lines were cultured according to ATCC propagation instructions. By following the procedure in Basappa et al. [37], first, 2×10^3 MCF-7 cells in 200 μL were grown in MEM enriched with 2% FBS and kept at 37 °C in a humidified 5% CO_2 environment. The compounds (10 mM) were dissolved in DMSO and were stored as a stock solution. The DMSO and the stock solution of compounds were diluted to 0.01, 0.1, 10, 100, and 1000 μM solutions in cell culture medium, keeping a DMSO amount less than 1%. MCF-7 cells (2×10^3) were incubated for 72 h with exposure to pyrimidines and Alamar Blue reagent was used to evaluate cell viability.

2.3. Annexin V Apoptosis and Cell Cycle Analysis Assay

MCF-7 cells were cultured at a density of approximately 1×10^5 cells per well on a six cm tissue culture petri dish, and treated with compounds **3a** or **5b** for 72 h. Following the procedure, attached and floating cells were gathered and rinsed twice with ice-cold phosphate buffer solution. The degree of apoptosis was determined using the Annexin V-AbFluor™ 488/PI Apoptosis Detection Kit (Abbkine, KTA0002, Wuhan, China) following the manufacturer's instructions. A quantity of 1×10^5 cells were collected, washed once in ice-cold PBS, and permeabilized with 100 μL of 0.5% Triton X-100 to evaluate cell cycle distribution. A quantity of 1×10^5 cells were fixed with 75% ethanol at -20 °C overnight and stained with 50 $\mu\text{g}/\text{mL}$ PI in 200 μL PBS supplemented with 20 $\mu\text{g}/\text{mL}$ (w/v) RNase A (Abbkine, KTA2020, Wuhan, China) for 1 h at 4 °C. Cytofluorometric acquisitions were performed on a BECKMAN COULER CytoFlex at a low flow rate mode.

2.4. Western Blot Analysis

MCF-7 cells were treated with compounds **3a** or **5b** and harvested, and the cell lysates were obtained. SDS-PAGE was used to separate the proteins of interest, and were transferred onto PVDF (Millipore, ISEQ00010, Burlington, MA, USA) membrane. The membrane was sequentially incubated with primary and secondary antibodies and the corresponding proteins were visualized using an ECL kit Clarity™ and Clarity Max™ Western ECL Blotting Substrates (BIO-RAD, Hercules, CA, USA).

2.5. Data Analysis and Statistics

The results are presented as mean \pm standard deviation. A one-way analysis of variance (one-way ANOVA), with Bonferroni's multiple comparison tests, was used to analyze the statistical change between treatment groups. A 0.05 confidence level was the significant change cutoff.

2.6. Molecular Docking

The docking studies were determined by using The Scripps Research Institute's AutoDock4 tools (v.1.5.6) [38]. Initially, **3a** or **5b** structures were obtained from the molecular drawing software tools, and the compounds were converted to the PDBQT format. Later protein preparation was performed by BIOVIA Discovery studio. Before this, the crystal structure of NF- κB (PDB ID: 1IKN) was retrieved from the Protein Data Bank. The protein structure was prepared by removing water molecules and adding hydrogen atoms.

Kollman charges were assigned to the protein. Later ligand preparations were performed for both compounds **3a** and **5b** and further used for docking purposes. Docking simulations were performed using AutoDock4. The Lamarckian Genetic Algorithm was employed for both ligands. The grid box was defined around the active site of the NF- κ B p65 subunit, and the grid dimensions were 40 Å × 40 Å × 28 Å with a spacing of 0.375 Å. The docking parameters were set to default values, and 10 docking runs were performed for each compound. Later, the resulting docking poses were visualized using BIOVIA Discovery Studio [39], PyMOL [40], and UCSF Chimera1.16 [41].

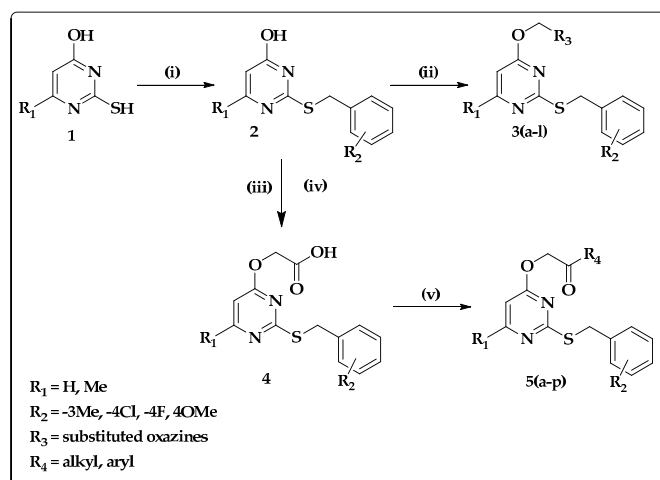
3. Results

3.1. Synthesis of Piperazine- and Oxazine-Linked Pyrimidine Derivatives

S-Benzylated of 2-thiouracil (**2**) was synthesized by refluxing substituted-2-thiouracil (**1**) and substituted benzyl chloride in EtOH:H₂O at basic conditions. Compound (**2**) was treated with substituted oxazine-bromides (**I**, **II**, **III**) in acetone under basic conditions, yielding thiouracil-oxazine hybrids **3(a-l)**. Also, refluxing compound (**2**) with *tert*-butylbromoacetate in DMF and further deprotection by TFA yielded compound (**4**). Compound **4** on acid-amine coupling with substituted piperazines (**IV**, **V**, **VI**, **VII**, and **VIII**) yielded derivatives **5(a-p)** (Scheme 1, Figure 2). All the synthesized compounds are characterised by spectroscopic technique (See supplementary file).

3.2. Efficacy of Pyrimidine Derivatives in Breast Cancer Cells

The newly synthesized pyrimidines were examined for inhibition of cell viability of human breast cancer (MCF-7) cells (Tables 1 and 2). Tamoxifen and doxorubicin were used as internal standards and produced a loss of viability of MCF-7 cells, with IC₅₀ values of 2.96 and 1.84 μM, respectively. Among the oxazine-clubbed pyrimidine compounds, **3a** and **3g** produced an IC₅₀ of 9.17 and 13.87 μM, respectively. Among piperazines, clubbed pyrimidine compounds **5a** and **5m** exhibited IC₅₀ of 6.29 and 14.58 μM. All other derivative IC₅₀ values were observed from 17.26 to >100 μM (Figure 3A) (see supplementary file). Among compounds **3(a-g)**, 4-methoxyphenyl-substituted oxazines (**I**) were observed to be active compared to 4-chlorophenyl and phenyl-substituted oxazines, whereas in compounds **5(a-p)**, 4-methoxybenzyl-substituted pyrimidine were more potent than other benzylated derivatives. Also, 5-bromopyridine-substituted piperazines were found to be active, whereas the other piperazines were inactive. Lead molecules **3a** and **5b** were evaluated against MDA-MB-231, BT-549, and SUM159PT cells (Figure 3B) (Table 3). Among the two oxazine-pyrimidine derivatives, **5b** was more potent, with IC₅₀ of 7.34, 5.98, and 14.81 μM.



Scheme 1. Synthesis of oxazine- and piperazine-clubbed pyrimidine. Reaction Conditions: (i) substituted benzyl chlorides (1.2 mmol), KOH (1.4 mmol), EtOH: H₂O (1:1), reflux; (ii) substituted oxazines (1.0 mmol), K₂CO₃ (2.0 mmol), acetone, reflux; (iii) *tert*-butylbromoacetate (1.2 mmol), K₂CO₃ (2.0 mmol), DMF, reflux; (iv) TFA, rt, (v) substituted amines, EDC.HCl, DMAP, Et₃N, DCM, rt.

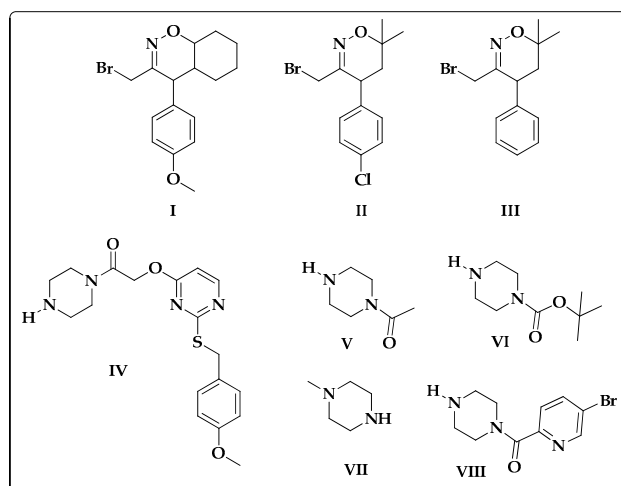


Figure 2. Structures of (I–VIII) substituent.

Table 1. Efficacy of newly synthesized oxazine-tethered thiouracil derivatives in MCF-7 cells.

Entry	R ₁	R ₂	R ₃	Yield in %	IC ₅₀ in μ M
3a	H	3Me	I	96	9.17
3b	H	3Me	II	96	>100
3c	H	3Me	III	95	22.68
3d	H	4Cl	I	94	23.53
3e	H	4Cl	II	91	>100
3f	H	4Cl	III	96	48.42
3g	H	4F	I	95	13.87
3h	H	4F	II	96	50.74
3i	H	4F	III	94	ND
3j	Me	4F	I	94	86.46
3k	Me	4F	II	96	ND
3l	Me	4F	III	97	ND
		Doxorubicin			2.96
		Tamoxifen			1.84

ND = Not Determined.

Table 2. Efficacy of newly synthesized piperazine-tethered thiouracil derivatives in MCF-7 cells.

Entry	R ₁	R ₂	R ₄	Yield in %	IC ₅₀ in μ M
5a	H	4OMe	IV	95	16.38
5b	H	4OMe	V	90	6.29
5c	H	4OMe	VI	90	17.26
5d	H	4OMe	VIII	94	29.38
5e	H	3Me	V	90	>100
5f	H	3Me	VII	80	79.00
5g	H	3Me	VI	89	>100
5h	H	3Me	VIII	90	30.09
5i	H	4F	VIII	89	83.30
5j	H	4F	V	95	>100
5k	H	4F	VII	85	>100
5l	H	4F	VI	80	>100
5m	H	4Cl	VIII	90	14.58
5n	H	4Cl	V	88	>100
5o	H	4Cl	VII	92	42.00
5p	H	4Cl	VI	80	>100
		Doxorubicin			2.96
		Tamoxifen			1.84

Table 3. IC₅₀ (μM) of lead molecules **3a** or **5b** in MDA–MB–231, BT–549, and SUM159PT cells.

Entry	MDA–MB–231	BT–549	SUM159PT
3a	7.34	5.98	14.81
5b	57.42	37.54	47.91

3.3. Title Compounds Induce Apoptosis in MCF–7 Cells

We previously described the discovery of 1,2 oxazines as anti-cancer drugs [32], along with their roles in triggering apoptosis, significantly increasing the population of sub-G1 cells and inhibiting the capacity of NF-κB to bind DNA in HCC cells. We therefore used MCF-7 cells to determine the effect of the lead compounds in Figure 4 on apoptosis. Examination of the data showed that the lead compounds stimulated dose-dependent apoptosis of MCF–7 cells (Figure 4).

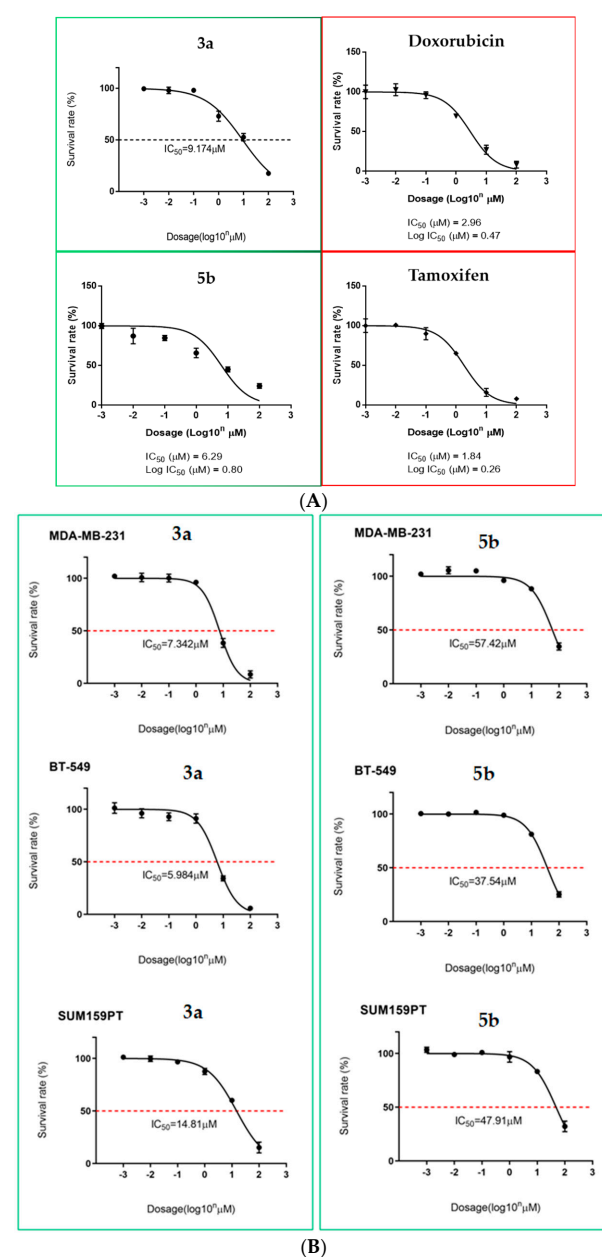


Figure 3. (A) IC₅₀ of compounds **3a**, **5b**, doxorubicin and tamoxifen in MCF-7 breast cancer cells. (B) Lead compounds, **3a** and **5b**, produce loss of cell viability in MDAMB231, BT–549 and SUM159PT cells. The IC₅₀ was calculated. Data represents triplicate determinations.

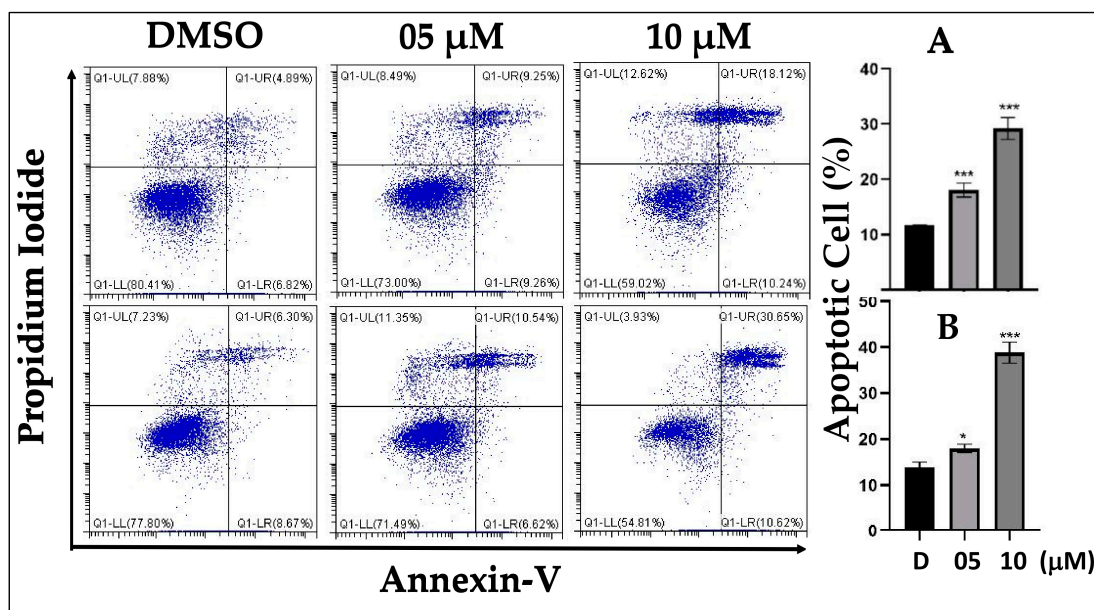


Figure 4. Evaluation of apoptosis in MCF-7 cells induced by lead compounds (5b, A and 3a, B) at 5 and 10 μM for 24 h. Control MCF-7 cells or MCF-7 cells treated with lead compounds (5b, A and 3a, B) were stained with Annexin V–AbFluor™ 488/PI Apoptosis Detection (Abbkine, KTA0002, Wuhan, China) followed by flow cytometry analysis. The percentage of apoptotic cells is indicated. Significant changes from the control group are shown by (* $p < 0.05$, *** $p < 0.01$) of three independent assays.

3.4. Lead Compounds Arrest MCF-7 Cell Cycle at the Sub-G1 Phase

We next investigated whether the lead compounds can hinder specific cell cycle progression. Propidium iodide labeling was used for the flow cytometric study of untreated and treated (lead compounds) MCF-7 cells. Lead compounds increased the proportion of cells in the sub-G1 phase relative to untreated cells [42] (Figure 5).

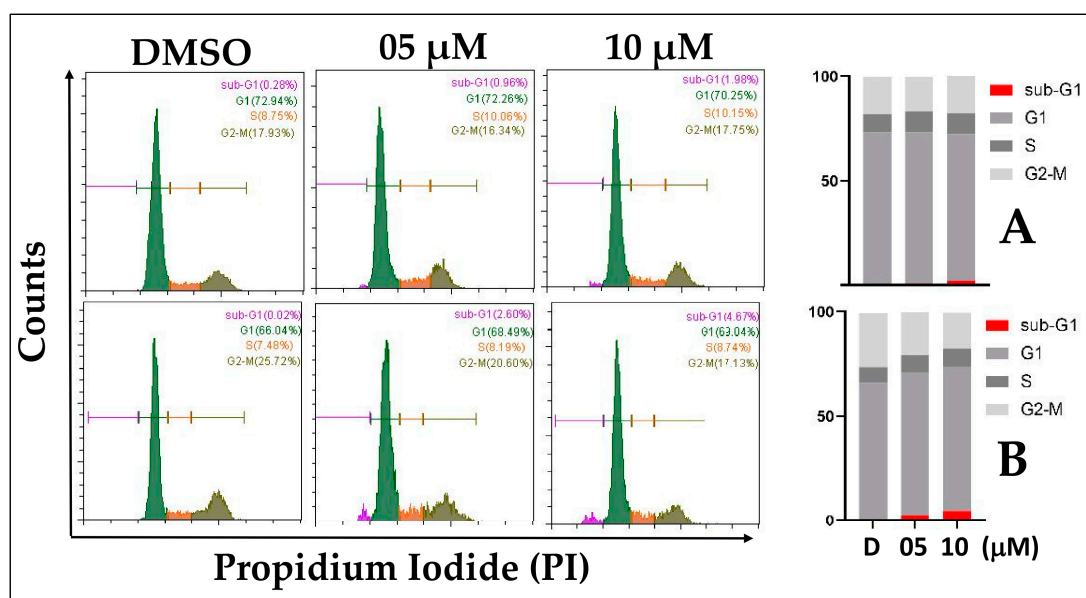


Figure 5. Flow cytometry analyzed MCF-7 cell cycle proportions. Representative cell cycle distribution histograms showing apoptosis in MCF-7 cells treated for 72 h with lead compounds such as A (5b) and B (3a) at concentrations of 5 and 10 mM, and analysis of the number of cells at each cell cycle stage with all phases.

3.5. Lead Compounds Inhibited the Phosphorylation of Human p65 Protein (Serine-536 Amino Acid) of NF- κ B Subunit in MCF-7 Cells

NF- κ B activation is regulated by the enzyme inhibitor of κ B (I κ B) and kinase (IKK), which phosphorylates subunit p65 at serine 536, and which inhibits the NF- κ B signaling pathway. Western blot analysis was used to examine if the lead compounds impacted the expression of the p65 protein or the levels of phospho-p65 in MCF-7 cells. Lead compounds **5b** and **3a**, as shown in Figure 6A,B, produce a concentration-dependent decrease of phospho-p65 levels relative to p65 protein expression in MCF-7 cells 24 h after treatment.

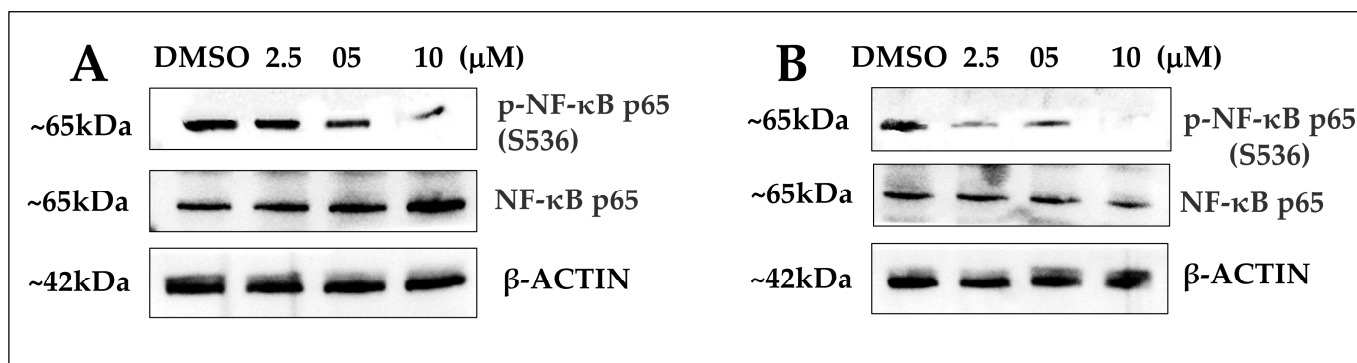


Figure 6. Effects of lead compounds **5b** (A) and **3a** (B) on the NF- κ B signaling pathway in MCF-7 cells. Cells were treated for 24 h with lead compounds (0–10 μ M). Western blotting evaluated p65 expression and phospho-p65 levels.

3.6. In Silico Analysis of Novel Compounds **3a** and **5b** Targeting the NF- κ B p65 Subunit

In this study, we performed in silico analysis to evaluate the binding energies and critical interactions of two novel compounds, **3a** or **5b**, targeting p65, the active site of NF- κ B. Initially, the NF- κ B structure was retrieved from the Protein Data Bank (PDB ID: 1IKN) and further used for molecular docking simulations using AutoDock4 tools. Molecular docking simulation revealed that novel compound **3a** demonstrated a binding energy of -9.32 kcal/mol, indicating a strong binding affinity for the active site of the NF- κ B p65 subunit, while **5b** exhibited a binding energy of -7.32 kcal/mol, indicating a relatively weaker binding affinity. Further key interactions revealed that compound **3a** formed a hydrogen bond with the residue GLN-29. The hydrogen bond plays a crucial role in stabilizing the binding of **3a** to the active site. One π -anion bond and one π -lone pair bond formed with the residues GLU-225 and GLU-222, respectively. Additionally, hydrophobic interactions (π -alkyl) were observed between **3a** and specific residues like LYS-28, ARG-30, ARG-50, and HIS-181 in the binding pocket, contributing to its overall binding affinity. In comparison, **5b** engaged in hydrogen bonding interactions with residues GLN-29 and ILE-224 within the active site. These hydrogen bonds contribute to the binding stability of **5b**. One π -sigma bond formed with the residue ARG-50. Furthermore, hydrophobic interactions were observed (LYS-28 and PRO-275), further enhancing the binding of **5b** to the target protein (Figure 7B). The results of the docking study revealed that both **3a** and **5b** have potential as inhibitors of the NF- κ B p65 subunit.

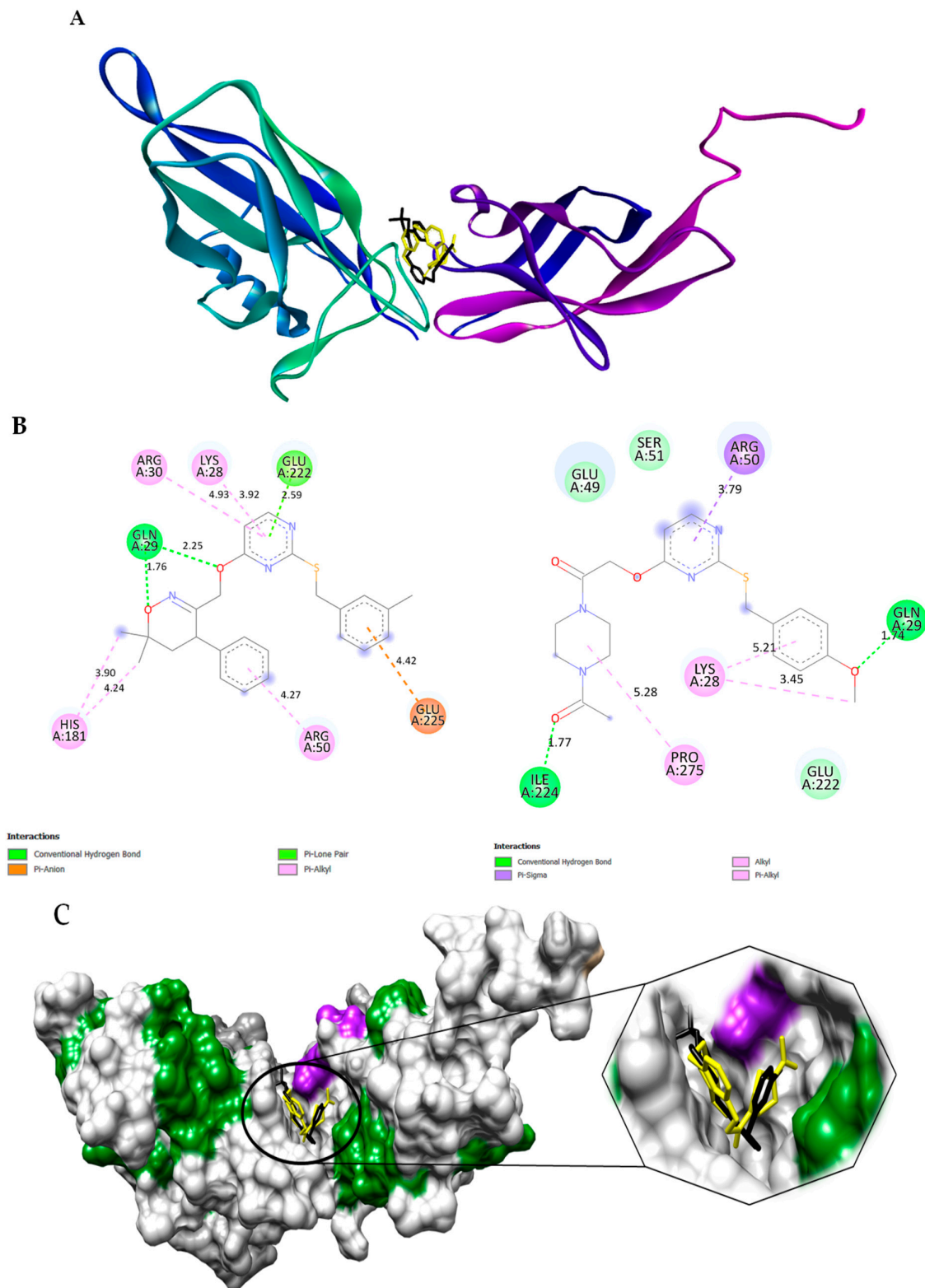


Figure 7. (A) Cartoon representation of both docked compounds **3a** (Black) and **5b** (Yellow) inside the binding pocket of the p65 subunit of NF- κ B; (B) 2D interactions of compound **3a** and **5b** with the walls of the binding pocket, respectively and showing bond distance (\AA) between respective amino acid and ligands. Pyrimidine ring of **3a** and 4-methoxybenzylthiol group of **5b** showed pi-alkyl interaction with Lys28 of p65 subunit of NF- κ B; (C) Representation of three-dimensional surface view of docked compounds (**3a**: Black, **5b**: Yellow) inside the groove of NF- κ B and its enlarged view for better understandings.

4. Discussion

Pyrimidines have been demonstrated to be effective inhibitors of NF- κ B, and many of the pyrimidine-based drugs such as ibudilast, spebrutinib, and dasatinib are also reported as inhibitors of the NF- κ B pathway. In the present work, we have designed and synthesized a new series of oxazine- and piperazine-clubbed pyrimidine derivatives as novel inhibitors of NF- κ B. Loss of cell viability in MCF-7 cells revealed **3a** and **5b** to be the most potent among the series. Further efficacy of the lead compounds was studied by apoptosis and cell cycle assays, and Western blot analysis. The lead compounds increased the proportion of cells in the sub-G1 phase relative to untreated cells and induced apoptosis in MCF-7 cells. Lead molecules **5b** and **3a** produced a concentration-dependent decrease of phospho-p65 levels in MCF-7 cells. Additionally, an in silico docking study of lead compounds also supported the above data by prediction of strong binding to the p65 subunit of NF- κ B.

5. Conclusions

In this study, novel compounds consisting of oxazines and piperazines linked to pyrimidines were synthesized and evaluated in MCF-7 breast cancer cells. Compounds **3a** and **5b** exhibited IC₅₀s of 9.17 and 6.29 μ M, respectively. Through in silico investigation, it was determined that compounds **3a** and **5b** potentially bind to the active site of NF- κ B. Subsequent biological assays confirmed that lead compounds **3a** and **5b** effectively inhibited NF- κ Bp65 phosphorylation in MCF-7 cells, presenting a promising chemical entity targeting NF- κ B in breast cancer cells.

Supplementary Materials: The following supporting information can be downloaded at: <https://www.mdpi.com/article/10.3390/biomedicines11102716/s1>. Figures S2–S23 and S24–S40 contain NMR, LCMS of **3(a–l)**, **5(a–p)**, and Figures S44–S50 contains IC₅₀ values of newly synthesized compounds.

Author Contributions: A.R., B.C.N., Z.X., D.V., A.M., P.G.C., K.S.A. and B.B.: conceptualization, methodology, and formal analysis; S.L.G., V.P., P.E.L. and B.B.: methodology, data curation and manuscript drafting. All authors have read and agreed to the published version of the manuscript.

Funding: This work was supported by the Vision Group on Science and Technology (CESEM) and the Government of Karnataka. This work was also supported by a Singapore MOE Tier 1 grant to GS. This work was supported by a National Research Foundation of Korea (NRF) grant funded by the Korean government (MSIP) (NRF-2021R111A2060024 and NRF-2022R111A1A01071593). This research was also supported by the National Natural Science Foundation of China (82172618); the Shenzhen Key Laboratory of Innovative Oncotherapeutics (ZDSYS20200820165400003) (Shenzhen Science and Technology Innovation Commission), China; Universities Stable Funding Key Projects (WDZC20200821150704001), China; The Shenzhen Bay Laboratory, Oncotherapeutics (21310031), China; Overseas Research Cooperation Project (HW2020008) (Tsinghua Shenzhen International Graduate School), China. A.R. thanks KSTePS, GOK, INDIA for providing the fellowship. B.C.N. thanks to OBC Cell, University of Mysore, Karnataka for the fellowship during this study.

Institutional Review Board Statement: Not applicable.

Informed Consent Statement: Not applicable.

Data Availability Statement: All data are freely available with this article.

Conflicts of Interest: The authors declare no conflict of interest.

References

1. Siegel, R.L.; Miller, K.D.; Jemal, A. Cancer Statistics, 2019. *CA A Cancer J. Clin.* **2019**, *69*, 7–34. [[CrossRef](#)] [[PubMed](#)]
2. Giaquinto, A.N.; Sung, H.; Miller, K.D.; Kramer, J.L.; Newman, L.A.; Minihan, A.; Jemal, A.; Siegel, R.L. Breast Cancer Statistics, 2022. *CA A Cancer J. Clin.* **2022**, *72*, 524–541. [[CrossRef](#)] [[PubMed](#)]
3. Sen, R.; Baltimore, D. Multiple Nuclear Factors Interact with the Immunoglobulin Enhancer Sequences. *Cell* **1986**, *46*, 705–716. [[CrossRef](#)] [[PubMed](#)]
4. Ghasemi, F.; Sarabi, P.Z.; Athari, S.S.; Esmailzadeh, A. Therapeutics Strategies against Cancer Stem Cell in Breast Cancer. *Int. J. Biochem. Cell Biol.* **2019**, *109*, 76–81. [[CrossRef](#)] [[PubMed](#)]

5. Zhang, J.; Zheng, J.; Chen, H.; Li, X.; Ye, C.; Zhang, F.; Zhang, Z.; Yao, Q.; Guo, Y. Curcumin Targeting NF- κ B/Ubiquitin-Proteasome-System Axis Ameliorates Muscle Atrophy in Triple-Negative Breast Cancer Cachexia Mice. *Mediat. Inflamm.* **2022**, *2022*, 2567150. [[CrossRef](#)] [[PubMed](#)]
6. Oeckinghaus, A.; Ghosh, S. The NF- κ B Family of Transcription Factors and Its Regulation. *Cold Spring Harb. Perspect. Biol.* **2009**, *1*, a000034. [[CrossRef](#)] [[PubMed](#)]
7. Zhang, Q.; Lenardo, M.J.; Baltimore, D. 30 Years of NF- κ B: A Blossoming of Relevance to Human Pathobiology. *Cell* **2017**, *168*, 37–57. [[CrossRef](#)]
8. Miller, S.C.; Huang, R.; Sakamuru, S.; Shukla, S.J.; Attene-Ramos, M.S.; Shinn, P.; Van Leer, D.; Leister, W.; Austin, C.P.; Xia, M. Identification of Known Drugs That Act as Inhibitors of NF- κ B Signaling and Their Mechanism of Action. *Biochem. Pharmacol.* **2010**, *79*, 1272–1280. [[CrossRef](#)]
9. Sun, X.-M.; Bratton, S.B.; Butterworth, M.; MacFarlane, M.; Cohen, G.M. Bcl-2 and Bcl-xL Inhibit CD95-Mediated Apoptosis by Preventing Mitochondrial Release of Smac/DIABLO and Subsequent Inactivation of X-Linked Inhibitor-of-Apoptosis Protein. *J. Biol. Chem.* **2002**, *277*, 11345–11351. [[CrossRef](#)]
10. Perkins, N.D.; Felzien, L.K.; Betts, J.C.; Leung, K.; Beach, D.H.; Nabel, G.J. Regulation of NF- κ B by Cyclin-Dependent Kinases Associated with the P300 Coactivator. *Science* **1997**, *275*, 523–527. [[CrossRef](#)]
11. Ding, L.; Cao, J.; Lin, W.; Chen, H.; Xiong, X.; Ao, H.; Yu, M.; Lin, J.; Cui, Q. The Roles of Cyclin-Dependent Kinases in Cell-Cycle Progression and Therapeutic Strategies in Human Breast Cancer. *Int. J. Mol. Sci.* **2020**, *21*, 1960. [[CrossRef](#)] [[PubMed](#)]
12. Baud, V.; Karin, M. Is NF- κ B a Good Target for Cancer Therapy? Hopes and Pitfalls. *Nat. Rev. Drug Discov.* **2009**, *8*, 33–40. [[CrossRef](#)] [[PubMed](#)]
13. Frantz, B.; O'Neill, E.A. The Effect of Sodium Salicylate and Aspirin on NF- κ B. *Science* **1995**, *270*, 2017–2018. [[CrossRef](#)] [[PubMed](#)]
14. Kopp, E.; Ghosh, S. Inhibition of NF- κ B by Sodium Salicylate and Aspirin. *Science* **1994**, *265*, 956–959. [[CrossRef](#)] [[PubMed](#)]
15. Mercogliano, M.F.; Bruni, S.; Elizalde, P.V.; Schillaci, R. Tumor Necrosis Factor α Blockade: An Opportunity to Tackle Breast Cancer. *Front. Oncol.* **2020**, *10*, 584. [[CrossRef](#)] [[PubMed](#)]
16. Chylińska, J.B.; Janowiec, M.; Urbański, T. Antibacterial Activity of Dihydro-1,3-Oxazine Derivatives Condensed with Aromatic Rings in Positions 5, 6. *Br. J. Pharmacol.* **1971**, *43*, 649–657. [[CrossRef](#)] [[PubMed](#)]
17. Zhang, R.-H.; Guo, H.-Y.; Deng, H.; Li, J.; Quan, Z.-S. Piperazine Skeleton in the Structural Modification of Natural Products: A Review. *J. Enzym. Inhib. Med. Chem.* **2021**, *36*, 1165–1197. [[CrossRef](#)] [[PubMed](#)]
18. Jalageri, M.D.; Nagaraja, A.; Puttaiahgowda, Y.M. Piperazine Based Antimicrobial Polymers: A Review. *RSC Adv.* **2021**, *11*, 15213–15230. [[CrossRef](#)]
19. Akl, L.; Abd El-Hafeez, A.A.; Ibrahim, T.M.; Salem, R.; Marzouk, H.M.M.; El-Domany, R.A.; Ghosh, P.; Eldehna, W.M.; Abou-Seri, S.M. Identification of Novel Piperazine-Tethered Phthalazines as Selective CDK1 Inhibitors Endowed with in Vitro Anticancer Activity toward the Pancreatic Cancer. *Eur. J. Med. Chem.* **2022**, *243*, 114704. [[CrossRef](#)]
20. Chen, Y.; Pan, W.; Ding, X.; Zhang, L.; Xia, Q.; Wang, Q.; Chen, Q.; Gao, Q.; Yan, J.; Lesyk, R.; et al. Design, Synthesis, and Anticancer Evaluation of Nitrobenzoxadiazole-Piperazine Hybrids as Potent pro-Apoptotic Agents. *Tetrahedron* **2023**, *138*, 133393. [[CrossRef](#)]
21. Walayat, K.; Mohsin, N.-A.; Aslam, S.; Ahmad, M. An Insight into the Therapeutic Potential of Piperazine-Based Anticancer Agents. *Turk. J. Chem.* **2019**, *43*, 1–23. [[CrossRef](#)]
22. Samie, N.; Muniandy, S.; Kanthimathi, M.S.; Haerian, B.S.; Raja Azudin, R.E. Novel Piperazine Core Compound Induces Death in Human Liver Cancer Cells: Possible Pharmacological Properties. *Sci. Rep.* **2016**, *6*, 24172. [[CrossRef](#)] [[PubMed](#)]
23. Rinne, M.; Mätlik, K.; Ahonen, T.; Vedovi, F.; Zappia, G.; Moreira, V.M.; Yli-Kauhaluoma, J.; Leino, S.; Salminen, O.; Kalso, E.; et al. Mitoxantrone, Pixantrone and Mitoxantrone (2-Hydroxyethyl)Piperazine Are Toll-like Receptor 4 Antagonists, Inhibit NF- κ B Activation, and Decrease TNF-Alpha Secretion in Primary Microglia. *Eur. J. Pharm. Sci.* **2020**, *154*, 105493. [[CrossRef](#)] [[PubMed](#)]
24. Deveshgowda, S.N.; Metri, P.K.; Shivakumar, R.; Yang, J.-R.; Rangappa, S.; Swamynayaka, A.; Shanmugam, M.K.; Nagaraja, O.; Madegowda, M.; Babu Shubha, P.; et al. Development of 1-(4-(Substituted)Piperazin-1-Yl)-2-((2-((4-Methoxybenzyl)Thio)Pyrimidin-4-Yl)Oxy)Ethanones That Target Poly (ADP-Ribose) Polymerase in Human Breast Cancer Cells. *Molecules* **2022**, *27*, 2848. [[CrossRef](#)] [[PubMed](#)]
25. Ramadass, V.; Vaiyapuri, T.; Tergaonkar, V. Small Molecule NF- κ B Pathway Inhibitors in Clinic. *Int. J. Mol. Sci.* **2020**, *21*, 5164. [[CrossRef](#)]
26. Mansouri, S.G.; Zali-Boeini, H.; Zomorodian, K.; Khalvati, B.; Pargali, R.H.; Dehshahri, A.; Rudbari, H.A.; Sahihi, M.; Chavoshpour, Z. Synthesis of Novel Naphtho [1,2-e][1,3]Oxazines Bearing an Arylsulfonamide Moiety and Their Anticancer and Antifungal Activity Evaluations. *Arab. J. Chem.* **2020**, *13*, 1271–1282. [[CrossRef](#)]
27. Yousif, M.N.M.; Fathy, U.; Yousif, N.M. Synthesis and Anticancer Activity of Novel Chromene Derivatives, Chromeno[2,3-d][1,3]Oxazines, and Chromeno[2,3-d]Pyrimidines. *Med. Chem.* **2023**, *19*, 578–585. [[CrossRef](#)]
28. Olivera, A.; Moore, T.W.; Hu, F.; Brown, A.P.; Sun, A.; Liotta, D.C.; Snyder, J.P.; Yoon, Y.; Shim, H.; Marcus, A.I.; et al. Inhibition of the NF- κ B Signaling Pathway by the Curcumin Analog, 3,5-Bis(2-Pyridinylmethylidene)-4-Piperidone (EF31): Anti-Inflammatory and Anti-Cancer Properties. *Int. Immunopharmacol.* **2012**, *12*, 368–377. [[CrossRef](#)]
29. Ananthula, S.; Parajuli, P.; Behery, F.; Ayoubi, A.; El Sayed, K.; Nazzal, S.; Sylvester, P. Abstract P3-03-11: Oxazine Derivatives of g- and D- Tocotrienols Display Potent Anticancer Effects in Vivo. *Cancer Res.* **2013**, *73*, P3-03. [[CrossRef](#)]

30. Ansari, N.; Khodagholi, F.; Amini, M.; Shaerzadeh, F. Attenuation of LPS-Induced Apoptosis in NGF-Differentiated PC12 Cells via NF- κ B Pathway and Regulation of Cellular Redox Status by an Oxazine Derivative. *Biochimie* **2011**, *93*, 899–908. [CrossRef]
31. Nirvanappa, A.C.; Mohan, C.D.; Rangappa, S.; Ananda, H.; Sukhorukov, A.Y.; Shanmugam, M.K.; Sundaram, M.S.; Nayaka, S.C.; Girish, K.S.; Chinnathambi, A.; et al. Novel Synthetic Oxazines Target NF- κ B in Colon Cancer In Vitro and Inflammatory Bowel Disease In Vivo. *PLoS ONE* **2016**, *11*, e0163209. [CrossRef] [PubMed]
32. Somu, C.; Mohan, C.D.; Ambekar, S.; Dukanya; Rangappa, S.; Baburajeev, C.; Sukhorukov, A.; Mishra, S.; Shanmugam, M.K.; Chinnathambi, A.; et al. Identification of a Novel 1,2 Oxazine That Can Induce Apoptosis by Targeting NF- κ B in Hepatocellular Carcinoma Cells. *Biotechnol. Rep.* **2020**, *25*, e00438. [CrossRef] [PubMed]
33. Mohan, C.D.; Bharathkumar, H.; Dukanya; Rangappa, S.; Shanmugam, M.K.; Chinnathambi, A.; Alharbi, S.A.; Alahmadi, T.A.; Bhattacharjee, A.; Lobie, P.E.; et al. N-Substituted Pyrido-1,4-Oxazin-3-Ones Induce Apoptosis of Hepatocellular Carcinoma Cells by Targeting NF- κ B Signaling Pathway. *Front. Pharmacol.* **2018**, *9*, 1125. [CrossRef] [PubMed]
34. Al-Khawaldeh, I.; Al Yasiri, M.J.; Aldred, G.G.; Basmadjian, C.; Bordoni, C.; Harnor, S.J.; Heptinstall, A.B.; Hobson, S.J.; Jennings, C.E.; Khalifa, S.; et al. An Alkynylpyrimidine-Based Covalent Inhibitor That Targets a Unique Cysteine in NF- κ B-Inducing Kinase. *J. Med. Chem.* **2021**, *64*, 10001–10018. [CrossRef] [PubMed]
35. Sun, Y.; Gao, Z.-F.; Yan, W.-B.; Yao, B.-R.; Xin, W.-Y.; Wang, C.-H.; Meng, Q.-G.; Hou, G.-G. Discovery of Novel NF- κ B Inhibitor Based on Scaffold Hopping: 1,4,5,6,7,8-Hexahydropyrido[4,3-d]Pyrimidine. *Eur. J. Med. Chem.* **2020**, *198*, 112366. [CrossRef] [PubMed]
36. Ha, H.-H.; Kim, J.S.; Kim, B.M. Novel Heterocycle-Substituted Pyrimidines as Inhibitors of NF- κ B Transcription Regulation Related to TNF- α Cytokine Release. *Bioorganic Med. Chem. Lett.* **2008**, *18*, 653–656. [CrossRef] [PubMed]
37. Basappa, B.; Chumadathil Pookunoth, B.; Shinduvalli Kempasiddegowda, M.; Knchugarakoppal Subbegowda, R.; Lobie, P.E.; Pandey, V. Novel Biphenyl Amines Inhibit Oestrogen Receptor (ER)- α in ER-Positive Mammary Carcinoma Cells. *Molecules* **2021**, *26*, 783. [CrossRef] [PubMed]
38. Huey, R.; Morris, G.M.; Olson, A.J.; Goodsell, D.S. A Semiempirical Free Energy Force Field with Charge-Based Desolvation. *J. Comput. Chem.* **2007**, *28*, 1145–1152. [CrossRef] [PubMed]
39. BIOVIA Dassault Systèmes. *Discovery Studio Visualizer*, 21.1.0.20298; Dassault Systèmes: San Diego, CA, USA, 2020.
40. Schrödinger, L.L.C.; DeLano, W. PyMOL. 2020. Available online: <http://www.pymol.org/pymol> (accessed on 15 February 2022).
41. Pettersen, E.F.; Goddard, T.D.; Huang, C.C.; Couch, G.S.; Greenblatt, D.M.; Meng, E.C.; Ferrin, T.E. UCSF Chimera—A Visualization System for Exploratory Research and Analysis. *J. Comput. Chem.* **2004**, *25*, 1605–1612. [CrossRef]
42. Parajuli, B.; Lee, H.-G.; Kwon, S.-H.; Cha, S.-D.; Shin, S.-J.; Lee, G.-H.; Bae, I.; Cho, C.-H. Salinomycin Inhibits Akt/NF- κ B and Induces Apoptosis in Cisplatin Resistant Ovarian Cancer Cells. *Cancer Epidemiol.* **2013**, *37*, 512–517. [CrossRef]

Disclaimer/Publisher’s Note: The statements, opinions and data contained in all publications are solely those of the individual author(s) and contributor(s) and not of MDPI and/or the editor(s). MDPI and/or the editor(s) disclaim responsibility for any injury to people or property resulting from any ideas, methods, instructions or products referred to in the content.